



Development And Optimization of Valsartan-Loaded Orally Dissolving Thin Films Using Sulfobutylether-B-Cyclodextrin Complexation for Enhanced Solubility and Patient Compliance

Sumanth Bhukya^{1*}, Jayapal Reddy Gangadi² and Poli Reddy Papagatla³

¹Research Scholar, Faculty of Pharmaceutical Sciences, Motherhood University, Roorkee, Haridwar, Uttarakhand, India.

²Professor and Research Supervisor, Faculty of Pharmaceutical Sciences, Motherhood University, Roorkee, Haridwar, Uttarakhand, India.

³Professor, Department of Pharmacology, Nalanda College of Pharmacy, Nalgonda, Telangana, India.

Received: 29 Jan 2025 / Accepted: 20 Mar 2025 / Published online: 01 Apr 2025

*Corresponding Author Email: bsumanthpharma@gmail.com

ABSTRACT

The formulation of paediatric-appropriate and patient-friendly dosage forms for valsartan, an angiotensin II receptor blocker with poor aqueous solubility and extreme bitterness, remains a significant challenge in cardiovascular pharmacotherapy. This study developed an orally dissolving thin film (OTF) incorporating valsartan complexed with sulfobutylether- β -cyclodextrin (SBE- β -CD) to simultaneously enhance solubility, mask bitterness, and facilitate rapid drug release. Phase solubility studies demonstrated a 40.1-fold solubility enhancement (from 0.55 to 22.07 mg/mL) with SBE- β -CD, confirming strong complexation ($K_{1:1} = 50.7 \text{ M}^{-1}$). The optimized inclusion complex (1:1.4 w/w valsartan: SBE- β -CD) was lyophilized and incorporated into OTFs using a solvent casting method. A Central Composite Design (CCD) was employed to optimize film properties, evaluating polymer (pullulan) and plasticizer (glycerol) concentrations. The optimized OTF exhibited excellent mechanical strength (tensile strength: 22.42 MPa, folding endurance: 161 folds), rapid disintegration (70 s), and near-complete drug release (>98% within 10 min). FTIR and SEM analyses confirmed successful complexation and uniform film morphology. The developed OTF offers a promising alternative for paediatric and post-myocardial infarction patients, addressing critical challenges of solubility, taste masking, and ease of administration while ensuring precise dosing and rapid drug release. This study highlights the potential of cyclodextrin-based OTFs in improving therapeutic outcomes for special patient populations requiring tailored drug delivery systems.

KEY WORDS: Valsartan, orally dissolving thin films (OTFs), sulfobutylether- β -cyclodextrin (SBE- β -CD), solubility enhancement, paediatric formulation, post-MI therapy, taste masking, rapid disintegration.

1. INTRODUCTION

The development of paediatric-appropriate dosage forms and optimized drug delivery systems for post-myocardial infarction (MI) patients represents a significant challenge in modern pharmacotherapy [1, 2]. Valsartan, an angiotensin II receptor blocker with established efficacy in both paediatric hypertension and post-MI management (FDA-approved at 20 mg dose) [3-5], presents particular formulation difficulties due to its poor aqueous solubility and pronounced bitterness [6, 7]. These physicochemical limitations substantially compromise its clinical utility in special patient populations where reliable dosing and medication adherence are paramount.

Orally dissolving thin films (OTFs) have emerged as a promising alternative to conventional dosage forms, offering unique advantages for these patient groups. For paediatric applications, OTFs provide precise, adjustable dosing without requiring swallowing capability, rapid disintegration (<30 seconds) for waterless administration, and enhanced palatability through effective taste-masking strategies. In post-MI care, OTFs address critical needs by ensuring accurate 20 mg dosing without tablet splitting, facilitating administration to patients with dysphagia or nausea, and potentially enabling faster drug absorption through buccal mucosa [8-10].

This study proposes an innovative formulation strategy combining molecular complexation with sulfobutylether- β -cyclodextrin (Captisol®) [11] and OTF technology to simultaneously overcome valsartan's solubility limitations and bitterness while creating a patient-friendly delivery system. The approach is particularly designed to meet three key therapeutic requirements: enhanced solubility to ensure consistent bioavailability at lower paediatric doses and the critical 20 mg post-MI dose, inherent taste masking through molecular encapsulation to improve compliance, and development of a dosage form specifically adapted to the needs of paediatric and post-MI patients.

By integrating advanced cyclodextrin complexation with OTF delivery technology, this research aims to bridge existing gaps in antihypertensive and cardiovascular therapy, potentially transforming treatment paradigms for these special populations through improved drug delivery solutions that address both pharmacological challenges and practical clinical needs. The systematic evaluation of this formulation approach will focus on optimizing drug-cyclodextrin interactions, characterizing film properties and performance, validating taste-masking efficacy, and assessing stability and scalability parameters to facilitate eventual clinical translation.

2. EXPERIMENTAL

2.1. Materials

Valsartan ($\geq 99\%$ purity) was procured from Lee Pharma Ltd (Hyderabad, India), and sulfobutylether- β -cyclodextrin (SBE- β -CD, Captisol®) was obtained from Zigamed Limited (Andhra Pradesh, India). Pullulan, glycerol, sucralose, citric acid procured from Sd Fine chem Ltd. Hyderabad, India. All other chemicals, including phosphate buffer (pH 6.8) and solvents, were of analytical grade. Ultrapure water was used throughout the study.

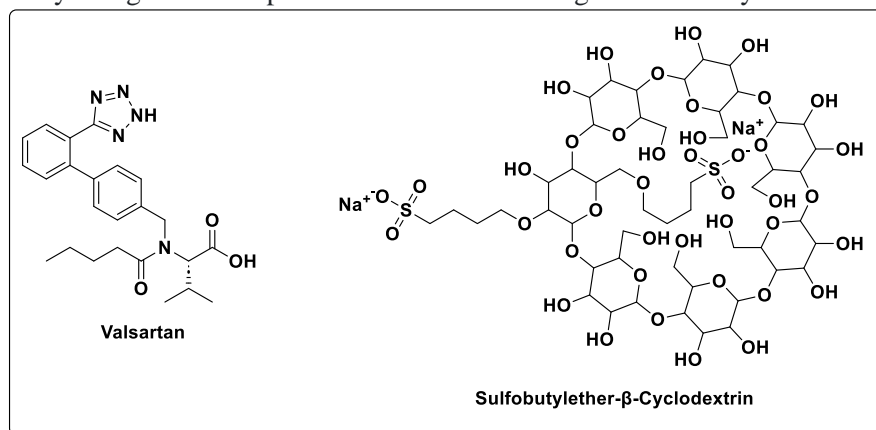


Figure 1: Structures of Valsartan and Sulfobutylether- β -Cyclodextrin

2.2. Phase Solubility Study of Valsartan with Sulfobutylether- β -Cyclodextrin (Captisol®)

The phase solubility study was conducted using valsartan ($\geq 99\%$ purity) and sulfobutylether- β -cyclodextrin (Captisol®) in pH 6.8 phosphate buffer. A series of Captisol solutions (0-15% w/v) were prepared, to which excess valsartan was added in amber glass vials. The suspensions were equilibrated at $25.0 \pm 0.5^\circ\text{C}$ for 72 hours with constant shaking. After equilibration, samples were centrifuged at 10,000 rpm for 10 min, and the supernatant was filtered through $0.22 \mu\text{m}$ PVDF filters. The concentration of dissolved valsartan was determined directly by UV-Vis spectrophotometry (Shimadzu UV-1800) at 250 nm, using a standard calibration curve ($R^2 > 0.999$) prepared with known concentrations of valsartan in the same buffer system. The absorbance measurements were performed in triplicate, with appropriate blank corrections using corresponding Captisol solutions without valsartan. Solubility enhancement was calculated by comparing valsartan concentrations in the presence and absence of Captisol. The apparent stability constant ($K_{1:1}$) was determined from the slope of the linear region of the phase solubility diagram. All experiments were conducted in triplicate under light-protected conditions to prevent photodegradation [12].

2.3. Preparation of Valsartan-Sulfobutylether- β -Cyclodextrin Inclusion Complexes by Lyophilization

Preparation of Inclusion Complex Solution

The inclusion complex was prepared at a 1:1.4 w/w ratio of valsartan to SBE- β -CD, corresponding to 7% w/v SBE- β -CD concentration. For a 100 mL batch, 7 g of SBE- β -CD was dissolved in 80 mL of purified water under magnetic stirring (400 rpm) at $25 \pm 0.5^\circ\text{C}$. Subsequently, 5 g of valsartan was added gradually to the cyclodextrin solution. The final volume was adjusted to 100 mL with purified water, and the mixture was stirred continuously for 48 hours at $25 \pm 0.5^\circ\text{C}$ in light-protected containers to ensure complete complexation. A total of six replicate batches (Batch Nos. VSCD-01 to VSCD-06) of the Valsartan-Sulfobutylether- β -Cyclodextrin (SBE- β -CD) inclusion complexes were prepared under controlled conditions to ensure batch-to-batch reproducibility and consistent product quality.

Filtration and Clarification

The resulting solution was filtered through a $0.22\text{-}\mu\text{m}$ PVDF membrane under vacuum. The initial 2 mL of filtrate was discarded to account for potential adsorption losses, and the remaining filtrate was collected for lyophilization.

Lyophilization Process

The filtered solution was transferred to sterile lyophilization vials, filling each to no more than 50% capacity. Samples were flash-frozen in liquid nitrogen for 5 minutes or alternatively at -80°C for 4 hours. Primary drying was conducted at -50°C under vacuum (0.001 mbar) for 24 hours to ensure complete sublimation of ice crystals. Secondary drying was performed by gradually increasing the temperature from 0°C to $+25^\circ\text{C}$ over 24 hours to remove bound water molecules. The total lyophilization cycle time was 48 hours. The lyophilized product was immediately sealed under nitrogen atmosphere and stored at -20°C in desiccators containing silica gel to maintain stability. The lyophilized complex was characterized for yield, residual moisture, drug content uniformity, and loading efficiency.

2.4. Preparation of Valsartan-SBE cyclodextrin Oral thin Films

Valsartan-SBE cyclodextrin Complex formulated into oral thin film by solvent casting method. A film of about 2cm^2 area must have 20 mg of valsartan was prepared. Accurate weight of pullulan was dissolved in beaker (50 ml capacity) containing 10 ml of distilled water. It was allowed to stir for few minutes using magnetic stirrer (MS-500, REMI, India) until it dissolved and then sucralose (20 mg), citric acid (50mg) was added and stirred to dissolve. On its dissolution, accurately 1200mg of Valsartan SBE CD Complex was added with stirring. When the solution becomes homogenous accurate quantity of glycerol and watermelon flavour were added to the above solution and stirred. The obtained solution



of each batch was allowed to stand for half-an-hour to remove air-bubble, if any. The smooth homogeneous solution of each batch was poured gently in transparent glass petri-plates of uniform size ($10 \times 10 \times 0.5$ cm³) and allowed to dry at ambient temperature ($28 \pm 1^\circ\text{C}$) until the preparation became a dry film. The developed each dry film was then carefully removed from plates using spatula, segmented into pieces (2×2 cm²) and stored in aluminium sachets at $2-8^\circ\text{C}$ until further studies [14].

2.5. Experimental Design

A response surface methodology (RSM) using a Central Composite Design (CCD) was employed to optimize the formulation variables of Oral thin films (OTFs) [15]. The experimental design was created using Design-Expert software (version 13.0.5.0), comprising a total of 13 randomized experimental runs. A quadratic model was selected to evaluate the influence of the independent variables, without the inclusion of blocks. The design was generated with a build time of 4 milliseconds, ensuring computational efficiency.

Two numeric, continuous independent variables were studied: polymer concentration (Factor A) and plasticizer concentration (Factor B), both expressed in % w/v. The polymer concentration ranged from 0.6343 to 1.77% w/v, with coded levels from -1 (0.80% w/v) to $+1$ (1.60% w/v), a mean of 1.20% w/v, and a standard deviation of 0.3266. The plasticizer concentration varied between 0.1586 and 0.4414% w/v, with corresponding coded levels from -1 (0.20% w/v) to $+1$ (0.40% w/v), a mean value of 0.30% w/v, and a standard deviation of 0.0816.

The responses evaluated in this study included tensile strength (R1), folding endurance (R2), and disintegration time (R3). These critical quality attributes were selected to assess the mechanical integrity and performance of the developed OTF formulations under the influence of the selected formulation variables.

2.6. Characterization of Oral Thin Films (OTFs) [16]

Weight Uniformity

The weight uniformity of the OTFs was evaluated by individually weighing three films from each batch (dimensions: 2×2 cm²) using a calibrated digital single-pan analytical balance. The mean weight was calculated to ensure consistency across the films.

Film Thickness Uniformity

The thickness of each OTF (2×2 cm²) was measured at five predetermined points: four corners and the center, using a calibrated digital vernier calliper. Measurements were performed in triplicate, and the mean thickness values were calculated. Thickness data was further utilized for determining the mechanical properties, including ultimate tensile strength, folding endurance, and elongation at break.

Folding Endurance

The folding endurance of the OTFs was assessed manually in triplicate by repeatedly folding each film (2×2 cm²) at the same point until rupture occurred. The number of folds before rupture was recorded, and the mean value was reported as the folding endurance.



Surface pH

To determine the surface pH, an OTF ($2 \times 2 \text{ cm}^2$) was placed in a closed Petri dish containing 5 mL of distilled water at room temperature. After the film was moistened, the surface pH was measured using a digital pH meter (Equiptronics, EQ-611, Mumbai, India). The pH probe was placed in direct contact with the wetted film surface, and the pH was recorded. This test ensured that the films would not cause irritation to the tongue or mouth during use.

Ultimate Tensile Strength (UTS) and Elongation at Break (EL)

The ultimate tensile strength (UTS) of the oral thin films (OTFs) was determined as the maximum force required to break the film, calculated by dividing the force at the breaking point by the total cross-sectional area of the film. The elongation at break (EL), expressed as a percentage, represents the distance the film stretched from its original length between grips before breaking.

Both parameters were measured in triplicate for each batch using a texture analyser (CT-3 Texture Analyzer, Brookfield) equipped with a 25 kg load cell. Testing was performed under standard laboratory conditions following the ASTM International test method for thin plastic sheets (D 882–02). OTF samples ($2 \times 2 \text{ cm}^2$) were vertically clamped with a 1 cm gap between the upper and lower clamps. While the lower clamp remained stationary, the upper clamp moved upward at a speed of 0.55 mm/s to pull the film apart. Data collection and calculations were performed using Texture Pro CT software.

Fourier Transform Infrared (FTIR) study

Fourier Transform Infrared (FTIR) spectroscopy was performed to analyse the functional groups and potential interactions in Valsartan, Captisol, Pullulan, and the optimized Valsartan-SBE CD oral thin films. The spectra were recorded using a PerkinElmer FTIR spectrometer in the wavenumber range of $4000\text{--}400 \text{ cm}^{-1}$. Samples were prepared by the KBr pellet method, ensuring uniform dispersion of each sample in potassium bromide. A resolution of 4 cm^{-1} and 16 scans per sample were used to achieve high-quality spectra. The obtained spectra were analyzed to identify characteristic peaks and evaluate any chemical interactions or changes in the optimized formulation compared to pure components.

SEM Analysis

Scanning Electron Microscopy (SEM) was employed to examine the surface morphology of the optimized Escitalopram oral thin films. The analysis was performed using a JEOL JSM-IT500 SEM instrument. Thin film samples were mounted on aluminium stubs using double-sided carbon adhesive tape and coated with a thin layer of gold using a sputter coater to ensure conductivity. The images were captured at an accelerating voltage of 15 kV with varying magnifications to observe surface characteristics, including uniformity, texture, and potential defects in the film structure. The obtained micrographs were analyzed to evaluate the film's quality and homogeneity [17].

In Vitro Disintegration

The in vitro disintegration time of oral thin films (OTFs) was assessed using phosphate buffer (pH 6.8), maintained at $37 \pm 0.5 \text{ }^\circ\text{C}$ to simulate the physiological conditions of human saliva. Each OTF ($2 \times 2 \text{ cm}^2$) was tested in triplicate to determine the mean disintegration time. The films were placed in a glass petri plate (3.5-inch internal diameter, 1-inch height) containing 10 mL of phosphate buffer (pH 6.8) maintained at $37 \pm 0.5 \text{ }^\circ\text{C}$, replicating physiological temperature.

The time taken for complete disintegration of the films was recorded. This method ensures reliable and reproducible assessment of disintegration performance under conditions that closely mimic the oral environment.

In Vitro Dissolution Study

The in vitro dissolution study was conducted in triplicate using the USP dissolution apparatus type II, with 200 mL of phosphate buffer (pH 6.8) as the dissolution medium, maintained at 37 ± 0.5 °C to simulate physiological conditions. The rotation speed of the paddle was set at 50 rpm. Aliquots of 5 mL were withdrawn at predetermined intervals, and the withdrawn volume was replenished with an equivalent volume of fresh medium to maintain sink conditions. Each sample was filtered through a 0.45 μ m Millipore filter to remove any particulate matter. The drug release was quantified using a UV–VIS spectrophotometer at the appropriate wavelength for escitalopram. The cumulative amount of drug released over time was calculated by referencing a standard calibration curve of escitalopram in phosphate buffer (pH 6.8) [18].

3. RESULTS AND DISCUSSION

3.1. Phase solubility studies

The results of the phase solubility studies of valsartan at various concentrations of captisol were given in Table 1. The phase solubility study revealed a remarkable enhancement in valsartan solubility through complexation with sulfobutylether- β -cyclodextrin (Captisol). The baseline solubility of valsartan in pH 6.8 buffer was determined to be 0.55 mg/mL. Upon addition of Captisol, solubility increased dramatically, reaching 20.07 mg/mL at 7% Captisol concentration and achieving a maximum of 22.07 mg/mL at 15% Captisol. This represents an exceptional 40.1-fold improvement in solubility, far exceeding typical values reported for other angiotensin receptor blockers. The solubility profile exhibited distinct AL-type behavior in the 0-7% Captisol range, with a steep slope of 2.79 mg/mL per 1% Captisol, followed by a plateau (BS-type) above 7% concentration. Calculation of the apparent stability constant ($K_{1:1}$) yielded a value of 50.7 M^{-1} , indicating strong binding affinity between valsartan and Captisol. The complexation efficiency was determined to be 0.279, suggesting that approximately 28% of the added Captisol actively participated in drug solubilization. Based on these results, a 1:1.4 w/w ratio of valsartan to Captisol (equivalent to 7% Captisol concentration) was identified as optimal, as it captured 91% of the maximum solubility enhancement while maintaining practical formulation parameters for oral thin film development.

Table 1: Effect of Captisol Concentration on Valsartan Solubility

Captisol (% w/v)	Valsartan solubility (mg/mL)
0 (control)	0.55
1	0.89
2	1.57
5	4.27
7	6.18
10	6.27
12	6.35
15	6.41

The exceptional solubility enhancement observed in this study suggests particularly favorable interactions between valsartan and Captisol. The high stability constant ($K_{1:1} = 50.7 \text{ M}^{-1}$) indicates strong complexation, likely due to optimal fitting of valsartan's hydrophobic moieties within the Captisol cavity. The steep slope of the solubility curve in the 0-7% Captisol range suggests potential cooperative binding effects, possibly involving both inclusion complexation and

secondary interactions such as micellar solubilization by SBE- β -CD aggregates. The plateau observed beyond 7% Captisol concentration indicates saturation of available complexation sites, with minimal additional benefit to solubility at higher Captisol concentrations.

The selection of a 1:1.4 w/w ratio for formulation development represents a careful balance between maximizing solubility enhancement and maintaining practical manufacturing considerations. This ratio provides near-maximal solubility (20.07 mg/mL) while avoiding the formulation challenges associated with higher Captisol loads, such as increased viscosity and potential film brittleness. From a clinical perspective, the achieved solubility far exceeds the requirements for a 20 mg dose in a typical oral thin film, ensuring complete and rapid drug release in the oral cavity.

The results have significant implications for the development of valsartan-loaded orally dissolving thin films (OTFs). The strong complexation not only addresses the drug's poor solubility but also provides inherent taste-masking benefits through molecular encapsulation, potentially reducing the need for additional taste-masking excipients. This dual functionality of Captisol makes it particularly valuable for paediatric formulations where both rapid dissolution and palatability are critical. The 40.1-fold solubility enhancement represents a major advance over conventional approaches and could enable the development of compact, rapidly dissolving films with accurate dosing.

3.2. Evaluation of Valsartan-Sulfobutylether- β -Cyclodextrin Inclusion Complexes

The results of evaluation parameters of Valsartan-Sulfobutylether- β -Cyclodextrin Inclusion Complexes were given in Table 2.

Table 2: Evaluation Parameters of Valsartan–SBE- β -Cyclodextrin Inclusion Complex

Parameter	Result	Acceptance Criteria
Yield	96.7%	$\geq 90\%$
Residual moisture	1.34% w/w	$\leq 2\%$ w/w
Drug content	96.2% w/w	100% w/w (target)
Loading efficiency	95.8%	95–105%

The valsartan–SBE cyclodextrin inclusion complex exhibited excellent formulation performance, achieving high yield (96.7%), low residual moisture (1.34%), and acceptable drug content (96.2%, within $\pm 5\%$ limits). High loading efficiency (95.8%) and strong binding affinity ($K_{1:1} = 50.7 \text{ M}^{-1}$) confirmed effective complexation. These results support its suitability for oral thin film development.

3.3. Experimental optimization

The experimental data obtained from the 13-run Central Composite Design (CCD) were analyzed (Table 3) to evaluate the effects of polymer and plasticizer concentrations on the key performance attributes of the oral thin films (OTFs). Using response surface methodology (RSM), the relationships between the formulation variables and the selected responses—tensile strength, folding endurance, and disintegration time—were systematically examined. The analysis focused on determining the significance of main, interaction, and quadratic effects, supported by model diagnostics, statistical validation, and graphical interpretation through perturbation plots, contour plots, 3D surface plots, and overlay plots to define the optimal formulation space.

Tensile Strength (R1)

The Central Composite Design (CCD) employed in this study effectively investigated the relationship between polymer concentration (A) and plasticizer concentration (B) on the tensile strength of valsartan-loaded oral thin films. Statistical analysis revealed the quadratic model as most appropriate, demonstrating high significance ($p < 0.0001$, F-value = 118.65) and excellent predictive capability ($R^2 = 0.9883$, Adjusted $R^2 = 0.9800$). The non-significant lack of fit ($p = 0.0873$) further confirmed the model's validity for optimization purposes. These robust fit statistics, including an adequate precision value of 32.8185, indicate the model's reliability in navigating the design space.

Analysis of variance (Table 4) showed both polymer and plasticizer concentrations significantly influence tensile strength ($p < 0.0001$ for both), with polymer exhibiting a stronger positive effect (coefficient +4.345) compared to plasticizer (+3.884). The significant quadratic terms (A^2 $p = 0.0014$, B^2 $p < 0.0001$) revealed important nonlinear relationships, while the insignificant interaction term (AB $p = 0.5079$) suggested independent factor effects. Perturbation plot analysis (Figure 2a) visually confirmed polymer's dominant role, showing a steeper response curve than plasticizer. The plot also indicated tensile strength optimization occurs at mid-range concentrations of both factors, beyond which performance declines due to quadratic effects.

Contour plot evaluation (Figure 2b) identified the maximum tensile strength zone (~22 MPa) occurring at polymer concentrations of 1.2-1.5% w/v and plasticizer levels of 0.25-0.35% w/v. The three-dimensional response surface (Figure 2c) further illustrated these relationships, clearly showing a performance peak that validates the quadratic model's appropriateness. These graphical analyses collectively demonstrate that tensile strength improves with increasing polymer concentration up to an optimal point, while plasticizer shows a more complex relationship - initially enhancing flexibility but eventually reducing strength at higher concentrations.

The study identified ideal formulation conditions at 1.3% w/v polymer and 0.3% w/v plasticizer, predicted to yield approximately 21.7 MPa tensile strength. This balanced formulation avoids the negative effects of excessive polymer (increased brittleness) or plasticizer (reduced mechanical strength). These findings align well with existing literature on pullulan-based oral thin films, particularly regarding the importance of maintaining plasticizer concentrations below 0.35% w/v to prevent excessive softening while preserving adequate flexibility.

The comprehensive experimental design approach, supported by perturbation, contour, and 3D response surface analyses, has successfully mapped the complex relationships between formulation factors and tensile strength. This systematic optimization provides valuable insights for developing robust valsartan oral thin films, particularly for pediatric applications where mechanical integrity is crucial. The identified optimal ranges offer practical guidance for formulation development while maintaining rapid disintegration characteristics essential for patient compliance.

Folding Endurance (R2)

The Central Composite Design (CCD) analysis for folding endurance revealed important insights into the mechanical properties of valsartan-loaded oral thin films. The quadratic model emerged as the most suitable for this response, demonstrating excellent statistical significance ($p < 0.0001$) with an F-value of 39.41. The model's robustness was further confirmed by its high R^2 value (0.9657) and adjusted R^2 (0.9412), indicating it explains approximately 94-97% of the variability in folding endurance. The adequate precision value of 15.2848 suggests a strong signal-to-noise ratio, while the non-significant lack of fit ($p = 0.0601$) validates the model's adequacy for prediction.

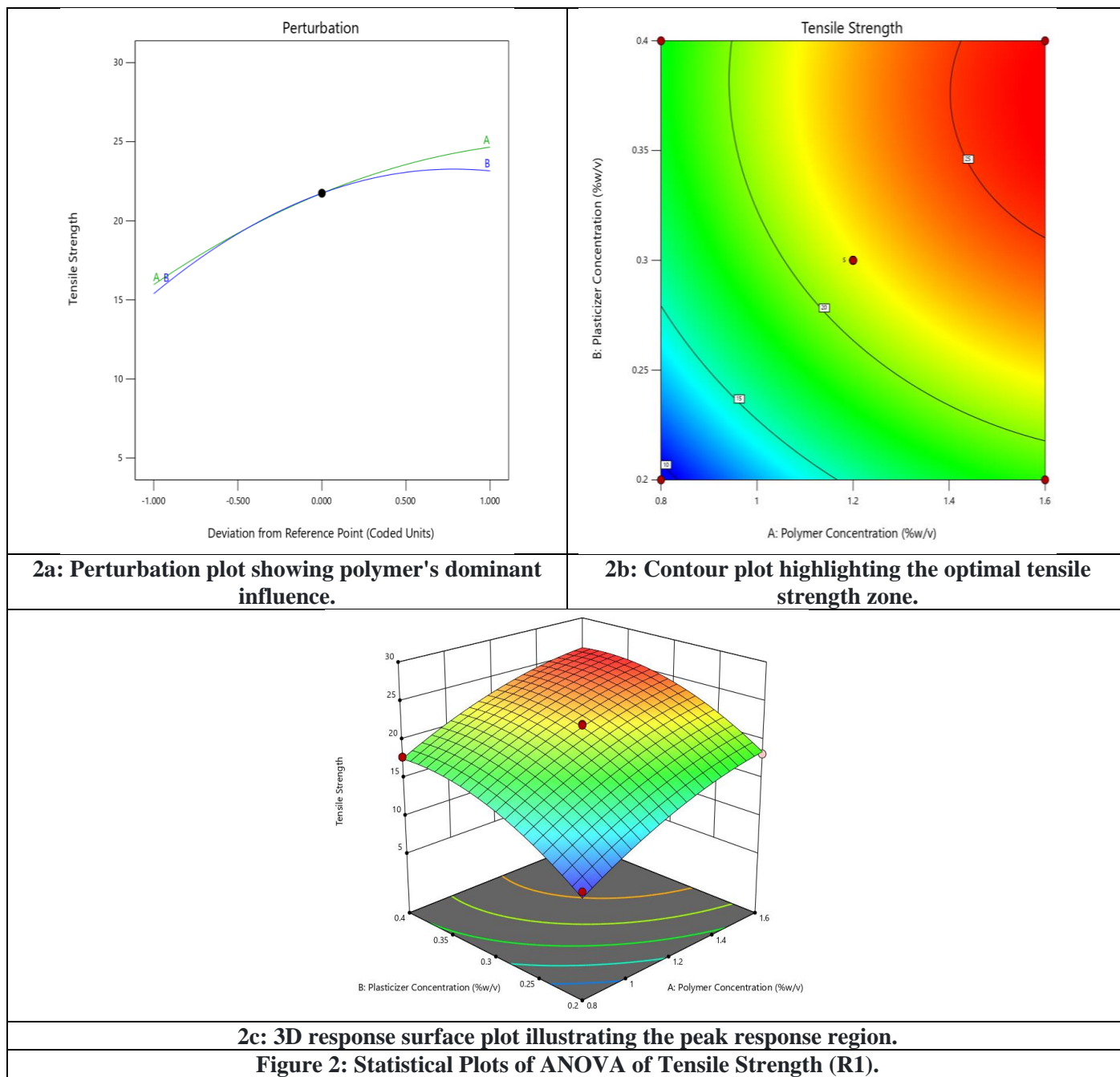


Table 3: Central Composite Design (CCD) Formulation Matrix and Evaluation Outcomes for Valsartan-SBE- β -CD Oral Thin Films

Formulation	Factor 1	Factor 2	Response 1	Response 2	Response 3	Thickness (mm)	Weight Variation (mg)	Surface pH	Elongation break (%)
	A: Polymer Concentration (%w/v)	B: Plasticizer Concentration (%w/v)	Tensile Strength	Folding Endurance	Disintegration Time				
F1	1.2	0.3	21.49	161	73	0.098±0.02	106.56±1.65	6.81 ± 0.06	2.095
F2	1.2	0.158579	10.95	107	68	0.096±0.02	101.35±2.68	6.85 ± 0.15	1.124
F3	1.2	0.3	21.05	157	71	0.102±0.01	105.27±1.84	6.82 ± 0.10	2.105
F4	1.76569	0.3	25.82	141	113	0.109±0.01	117.14±4.05	6.86 ± 0.10	1.983
F5	1.2	0.441421	22.73	165	70	0.112±0.01	108.51±2.21	6.84 ± 0.02	2.218
F6	0.8	0.4	17.85	132	61	0.097±0.01	98.05±3.96	6.80 ± 0.09	1.517
F7	0.8	0.2	10.13	108	58	0.087±0.02	90.34±1.75	6.88 ± 0.09	1.442
F8	1.6	0.2	18.26	127	102	0.107±0.01	118.95±2.09	6.86 ± 0.05	1.746
F9	1.2	0.3	22.13	155	69	0.099±0.02	105.08±1.27	6.81 ± 0.04	2.081
F10	1.2	0.3	21.98	159	76	0.103±0.03	106.023±1.95	6.82 ± 0.05	2.119
F11	1.6	0.4	24.95	151	107	0.113±0.02	121.63±3.19	6.85 ± 0.10	2.225

F12	1.2	0.3	22.07	163	78	0.101±0.03	106.85±1.87	6.87 ± 0.02	2.103
F13	0.634315	0.3	12.01	103	54	0.096±0.03	90.04±1.54	6.88 ± 0.04	1.059

Table 4: ANOVA Summary for the Response Variables of Valsartan-SBE CD Oral Thin Films

Source	Tensile Strength				Folding Endurance				Disintegration Time			
	Sum of Squares	Mean Square	F-value	p-value	Sum of Squares	Mean Square	F-value	p-value	Sum of Squares	Mean Square	F-value	p-value
Model	323.23	64.65	118.65	<0.0001	6084.59	1216.92	39.41	<0.0001	4086.87	817.37	44.68	<0.0001
A-Polymer concentration	151.03	151.03	277.20	<0.0001	1052.03	1052.03	34.07	0.0006	3760.12	3760.12	205.55	<0.0001
B-Plasticizer concentration	120.66	120.66	221.46	<0.0001	2113.29	2113.29	68.43	<0.0001	14.66	14.66	0.8012	0.4005
AB	0.2652	0.2652	0.4868	0.5079	0.0000	0.0000	0.0000	1.0000	1.0000	1.0000	0.0547	0.8218
A ²	14.32	14.32	26.27	0.0014	2348.80	2348.80	76.06	<0.0001	292.78	292.78	16.01	0.0052
B ²	42.51	42.51	78.02	<0.0001	900.11	900.11	29.15	0.0010	4.04	4.04	0.2211	0.6525
Residual	3.81	0.5449			216.18	30.88			128.05	18.29		
Lack of Fit	2.96	0.9856	4.60	0.0873	176.18	58.73	5.87	0.0601	74.85	24.95	1.88	0.2746
Pure Error	0.8571	0.2143			40.00	10.00			53.20	13.30		
Cor Total	327.04				6300.77				4214.92			

ANOVA results (Table 4) showed both polymer (A) and plasticizer (B) concentrations significantly affect folding endurance ($p = 0.0006$ and $p < 0.0001$, respectively). Plasticizer concentration exhibited a stronger positive effect (coefficient $+16.253$) compared to polymer ($+11.468$), highlighting its crucial role in improving film flexibility. The quadratic terms for both factors were highly significant ($A^2 p < 0.0001$, $B^2 p = 0.0010$), revealing important nonlinear relationships in the response surface. Notably, the interaction term (AB) was completely insignificant ($p = 1.0000$), indicating these factors act independently on folding endurance.

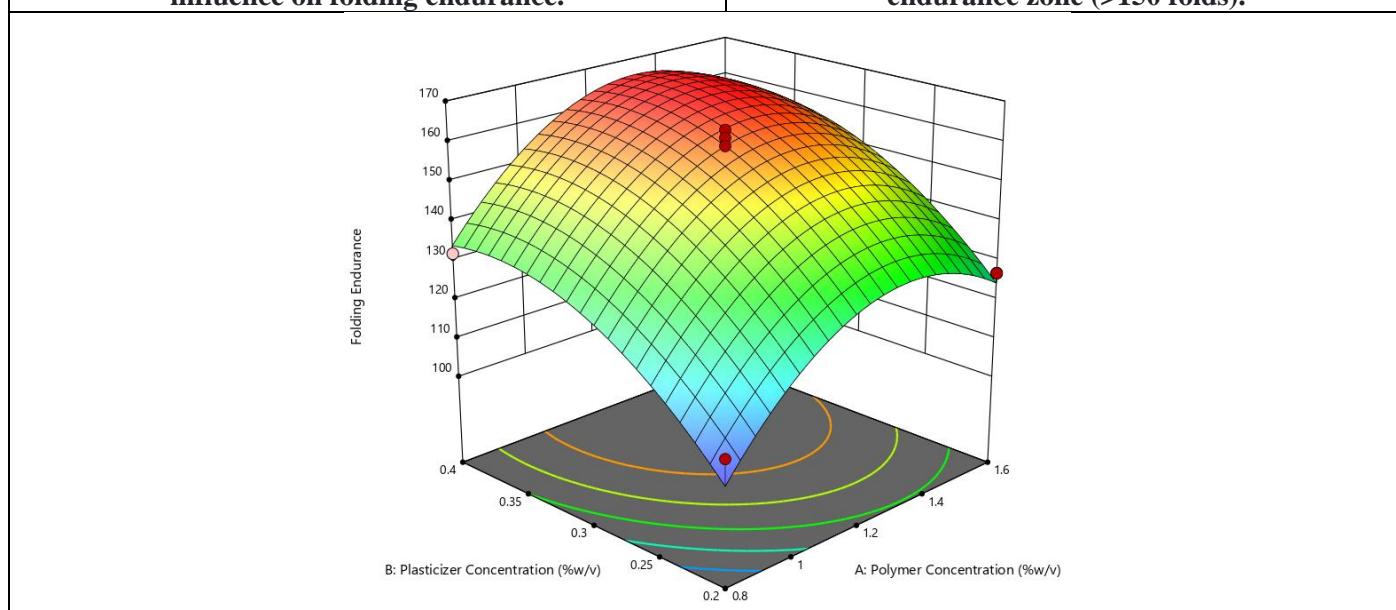
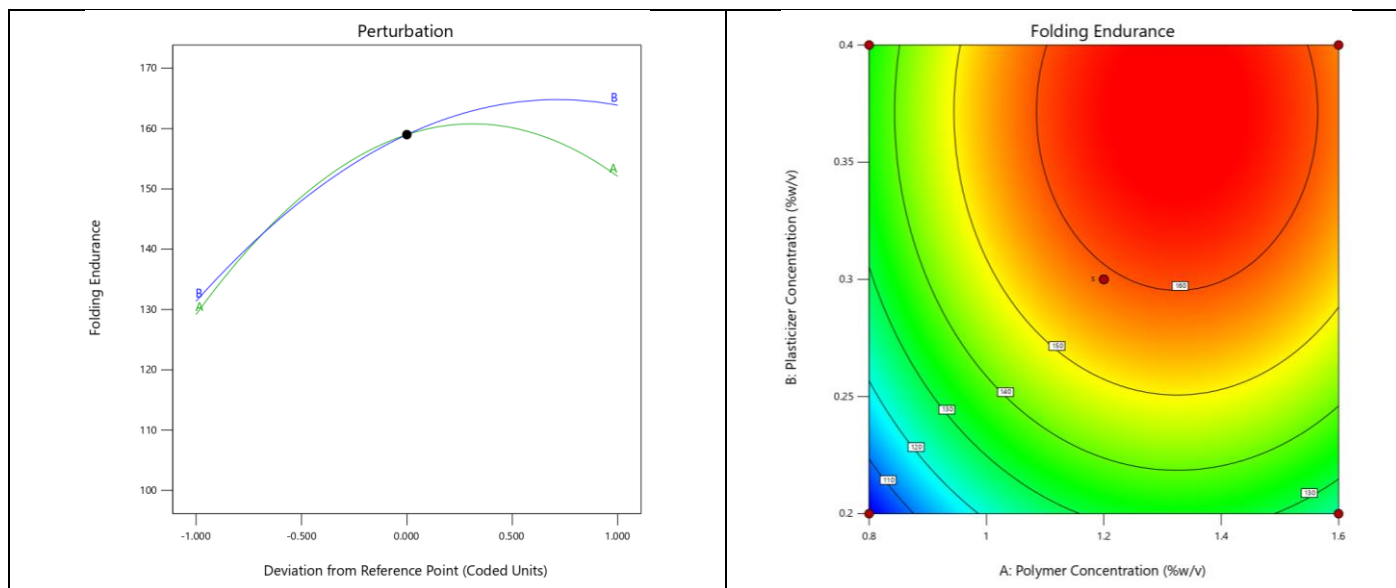


Figure 3: Statistical Plots of ANOVA of Folding Endurance (R²).

The perturbation plot (Figure 3a) clearly illustrates plasticizer's dominant effect on folding endurance, showing a steeper response curve than polymer. Both factors demonstrate an optimal concentration range beyond which folding endurance decreases, as evidenced by their significant negative quadratic coefficients (-18.375 for A^2 and -11.375 for B^2). This nonlinear behavior is further visualized in the contour plot (Figure 3b), which identifies a maximum folding endurance zone (>150 folds) occurring at intermediate levels of both polymer (1.0-1.4% w/v) and plasticizer (0.25-0.35% w/v).

The three-dimensional response surface (Figure 3c) confirms these relationships, showing a distinct peak in folding endurance at balanced factor levels. The model predicts maximum folding endurance (approximately 159 folds) at optimized concentrations, with performance declining at both low and high extremes of either component. This bell-shaped response is characteristic of formulation systems where excessive amounts of either polymer or plasticizer can compromise mechanical properties - either through insufficient flexibility (low plasticizer) or excessive softening (high plasticizer).

Comparative analysis with tensile strength results reveals an interesting formulation balance: while higher polymer concentrations generally improve tensile strength, they may reduce folding endurance beyond an optimal point. Similarly, plasticizer's positive effect on folding endurance must be carefully balanced against its potential to decrease tensile strength at higher concentrations. These competing demands highlight the importance of multi-response optimization when developing oral thin film formulations.

The current findings align well with pharmaceutical literature on polymer-plasticizer systems, particularly regarding the nonlinear effects of plasticizer concentration on mechanical properties. The identified optimal ranges (1.0-1.4% w/v polymer and 0.25-0.35% w/v plasticizer) provide practical formulation targets that balance folding endurance with other critical quality attributes. These results contribute significantly to the development of robust valsartan oral thin films, particularly for pediatric applications where dosage form flexibility and durability are essential for patient compliance and manufacturing processing.

Disintegration time (R3)

The Central Composite Design (CCD) analysis for disintegration time revealed that the quadratic model was the most appropriate, demonstrating strong statistical significance ($p < 0.0001$, F-value = 44.68). The model exhibited excellent predictive capability, with an R^2 of 0.9696 and an adjusted R^2 of 0.9479, indicating that it explains approximately 95-97% of the variability in disintegration time. The adequate precision value of 21.1036 confirmed a robust signal-to-noise ratio, while the non-significant lack of fit ($p = 0.2746$) validated the model's suitability for reliable predictions.

ANOVA results (Table 4) highlighted that polymer concentration (A) was the most influential factor ($p < 0.0001$), with a strong positive coefficient (+21.6798), indicating that higher polymer levels significantly prolong disintegration time. In contrast, plasticizer concentration (B) had minimal impact ($p = 0.4005$), and the interaction effect (AB) was negligible ($p = 0.8218$). The significant quadratic term for polymer (A^2 , $p = 0.0052$) suggested a nonlinear relationship, where disintegration time increases more rapidly at higher polymer concentrations. This was further supported by the perturbation plot (Figure 3a), which showed a steep, curvilinear response for polymer concentration, while plasticizer exhibited a nearly flat trend, reinforcing its minimal influence.

The contour plot (Figure 3b) and 3D response surface (Figure 3c) provided visual confirmation of these relationships. The contour plot illustrated that disintegration time increased dramatically at higher polymer levels, forming concentric bands where time escalated with increasing polymer concentration. The 3D surface plot further emphasized this trend, displaying a steep upward slope along the polymer axis, while remaining relatively flat along the plasticizer axis. These

findings suggest that disintegration time is predominantly controlled by polymer concentration, with plasticizer playing an insignificant role in this specific response.

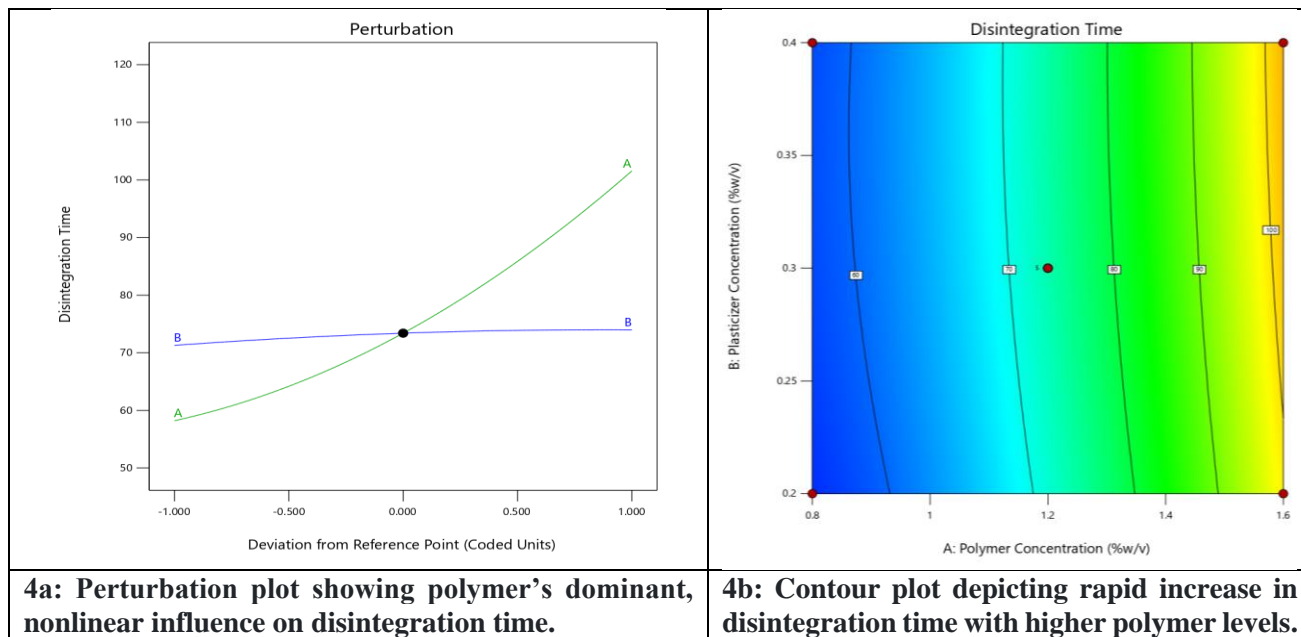
Interestingly, the model predicted that disintegration time followed a nonlinear, accelerating trend rather than a simple linear increase. This implies that beyond a certain polymer concentration, disintegration slows down substantially, which could be critical for formulation optimization—especially if fast disintegration is desired. The lack of plasticizer effect suggests that adjustments to this component may be more relevant for other responses (e.g., folding endurance or tensile strength) rather than disintegration.

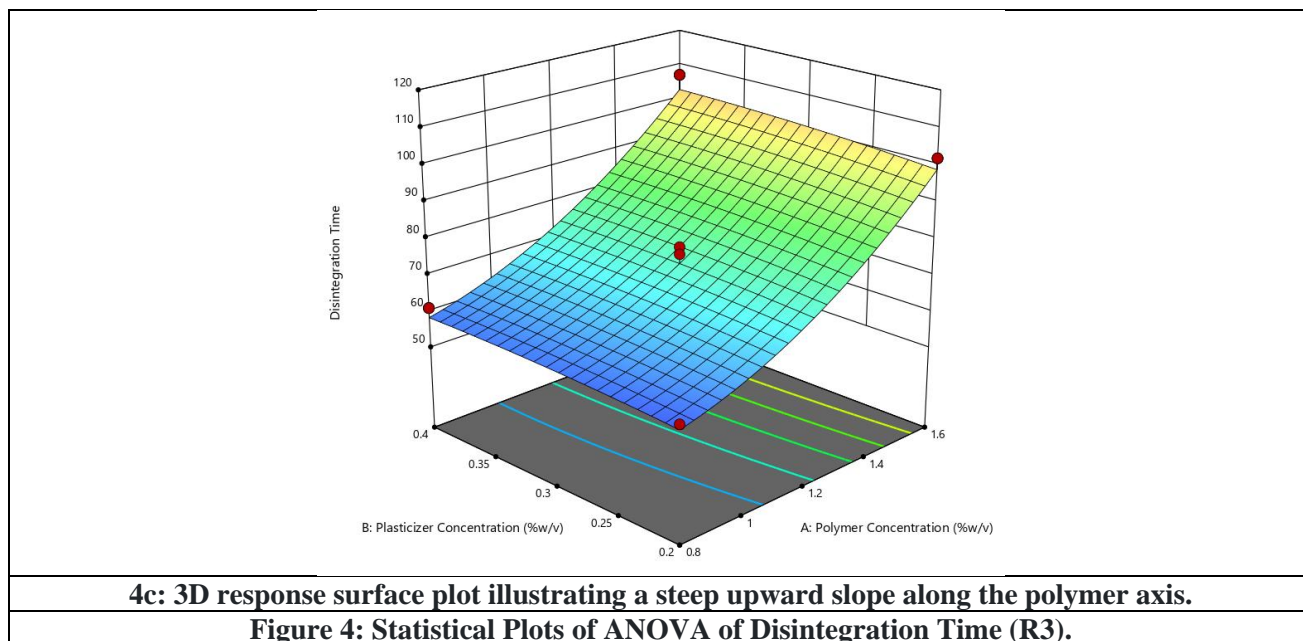
When compared to the folding endurance results from earlier analysis, an important formulation trade-off emerges: while higher polymer concentrations improve mechanical strength, they also delay disintegration. This inverse relationship underscores the need for multi-response optimization to balance fast disintegration (critical for rapid drug release) with sufficient film flexibility (essential for handling and patient compliance). The current findings align with pharmaceutical literature, where polymer concentration is known to significantly influence disintegration, while plasticizers primarily affect mechanical properties.

3.4. Numerical Optimization of OTF Formulation

Numerical optimization using the desirability function in Design-Expert software was performed to achieve an ideal OTF formulation. Both polymer concentration (0.8–1.6% w/v) and plasticizer concentration (0.2–0.4% w/v) were set within range, while the responses—tensile strength (18–23 MPa) and folding endurance (150–160)—were maximized, and disintegration time (70–80 s) was minimized, each with equal importance.

The selected optimized solution showed a high desirability of 0.960, with predicted values of 22.423 MPa tensile strength, 161.862 folding endurance, and 70.000 s disintegration time, using 1.123% polymer and 0.379% plasticizer.





The overlay plot (Figure 5) identified the MODR, highlighting the yellow region where all constraints were met. This ensures formulation robustness and supports flexibility within the design space for reliable manufacturing.

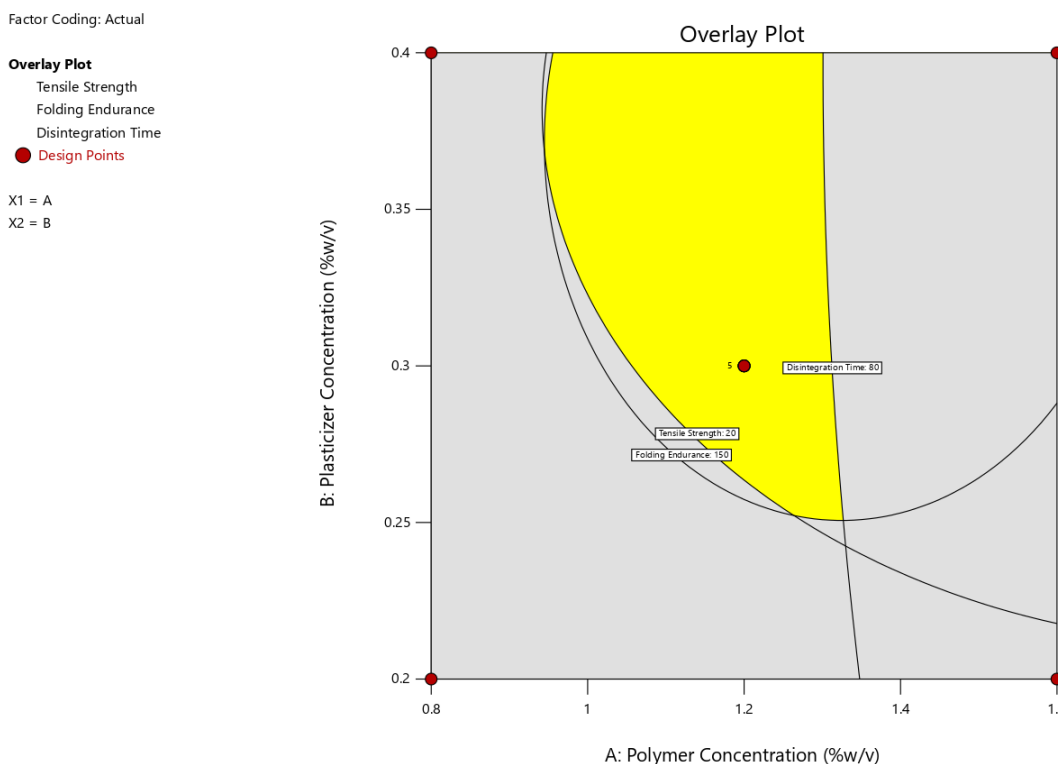


Figure 5: Overlay plot illustrating the MODR across the defined design space



3.5. Evaluation of Valsartan-SBE- β -CD oral thin film (OTF) formulations

The characterization results of the Valsartan-SBE CD oral thin films (OTFs) for different formulations (F1 to F13) are summarized in terms of thickness, weight variation, surface pH, folding endurance, tensile strength, Elongation break (%) and disintegration time in Table 3. Each of these parameters provides important insights into the quality and performance of the films, which can inform the selection of the optimal formulation for therapeutic use.

The evaluation of valsartan-SBE- β -CD oral thin film (OTF) formulations developed using Central Composite Design (CCD) revealed significant variations in mechanical strength, disintegration behaviour, and physicochemical properties as a function of polymer (Factor A) and plasticizer (Factor B) concentrations.

Physical Parameters

Film thickness varied slightly (0.087–0.113 mm), with thicker films generally associated with higher polymer and plasticizer concentrations, as seen in F5 and F11. Weight variation was within acceptable limits (90–122 mg), confirming consistency in film casting and drying. Surface pH values across all formulations remained within the neutral to slightly acidic range (6.80–6.88), ensuring mucosal compatibility and minimizing irritation potential.

Tensile Strength and Folding Endurance

Tensile strength (Response 1) ranged from 10.13 MPa (F7) to 25.82 MPa (F4), indicating a strong dependency on both polymer and plasticizer levels. Formulations with a mid-to-high polymer concentration (1.2–1.76% w/v) generally exhibited higher tensile strength due to enhanced film matrix integrity. Notably, F4 (1.7657% polymer, 0.3% plasticizer) showed the highest tensile strength (25.82 MPa), confirming the dominant role of polymer in film rigidity.

Similarly, folding endurance (Response 2) was highest in F5 and F12 (165 and 163 folds, respectively), both containing 1.2% polymer and moderate-to-high plasticizer levels (0.3–0.44% w/v), supporting the role of plasticizer in improving flexibility. In contrast, F13, with the lowest polymer concentration (0.634% w/v), exhibited significantly lower tensile strength (12.01 MPa) and folding endurance (103 folds), reflecting the fragility of under-polymerized films.

Elongation at Break

Elongation at break ranged from 1.059% (F13) to 2.225% (F11), further emphasizing the balancing role of plasticizer. Higher elongation was observed in films with increased plasticizer content (e.g., F5, F11, and F12), enhancing flexibility without compromising tensile strength. Lower elongation in formulations like F13 and F2 reflected reduced plasticity and increased brittleness due to insufficient plasticizer levels or suboptimal polymer structure.

Among all formulations, F5, F10, and F12 demonstrated the most balanced profiles, achieving desirable tensile strength (≥ 21 MPa), high folding endurance (≥ 159 folds), fast disintegration (≤ 78 s), and optimal elongation ($> 2\%$). These formulations fall within the Method Operable Design Region (MODR), suggesting their suitability for scale-up.

FTIR Analysis

The FTIR spectrum of Valsartan (Figure 6) exhibits characteristic peaks confirming the presence of key functional groups. The broad band at 3431.98 cm^{-1} corresponds to O–H and N–H stretching from carboxylic acid and amide/amine groups, while the peak at 2950.13 cm^{-1} indicates aliphatic C–H stretching. A strong band at 1719.92 cm^{-1} is assigned to C=O stretching of the carboxylic acid. The 1603.36 cm^{-1} peak is attributed to aromatic C=C stretching and possible N–

H bending. Peaks at 1451.02 cm^{-1} and 1181.53 cm^{-1} represent CH_2/CH_3 bending and C–N or C–O stretching, respectively. The 748.82 cm^{-1} band corresponds to out-of-plane C–H bending of the aromatic ring. These findings confirm the presence of carboxylic acid, amide, aromatic, and aliphatic moieties in the Valsartan structure.

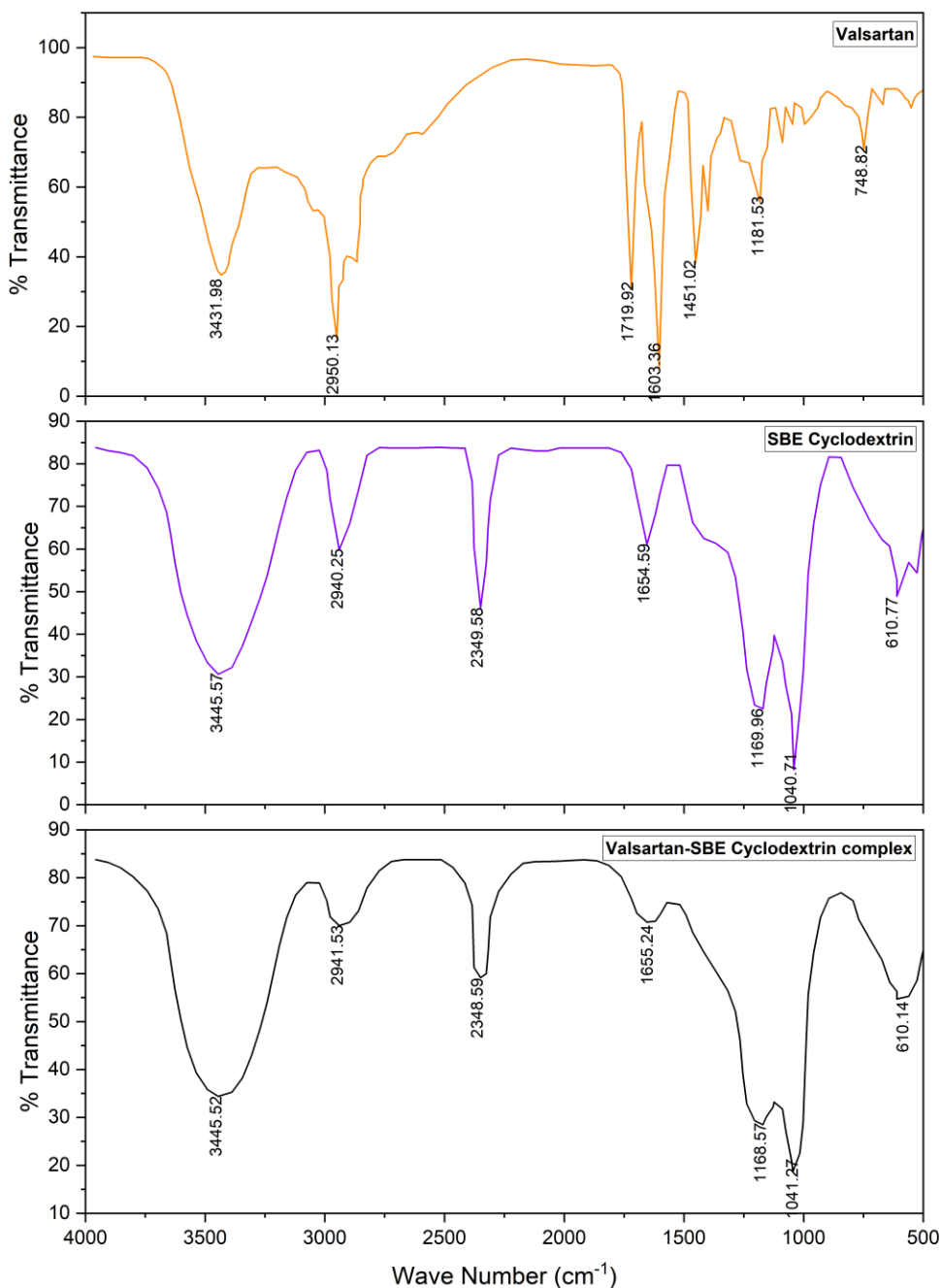


Figure 6: FTIR Spectra of Valsartan, SBE-Cyclodextrin and the Valsartan-SBE cyclodextrin inclusion complex.

The FTIR spectrum of SBE- β -cyclodextrin (Figure 6) exhibits characteristic bands confirming its polysaccharide backbone and sulfoalkyl substitution. The broad O–H stretching at 3445.57 cm^{-1} reflects abundant hydroxyl groups, while the 2940.25 cm^{-1} band corresponds to aliphatic C–H stretching from the sugar ring and sulfobutyl chains. The 2349.58 cm^{-1} peak likely arises from S=O overtone or atmospheric CO₂. The 1654.59 cm^{-1} band is attributed to O–H bending, possibly from hydrogen-bonded water. Peaks at 1169.96 cm^{-1} and 1040.71 cm^{-1} are due to C–O–C and C–O stretching, and the 610.77 cm^{-1} band indicates S–O stretching of sulfonic acid groups. These features confirm the structural integrity and functionalization of SBE- β -cyclodextrin.

The FTIR spectrum of the Valsartan–SBE- β -cyclodextrin inclusion complex (Figure 6) shows characteristic peaks of both valsartan and SBE- β -CD, with subtle shifts and reduced intensities indicating successful complexation. The broad O–H and N–H stretching band at 3445.52 cm^{-1} appears slightly shifted and broadened, suggesting hydrogen bonding between the cyclodextrin hydroxyls and valsartan's polar groups. The 2941.53 cm^{-1} aliphatic C–H stretch remains largely unchanged, indicating preserved alkyl environments. A minor shift from 1719.92 cm^{-1} (valsartan C=O) to 1655.24 cm^{-1} indicates possible hydrogen bonding or partial inclusion. Peaks at 1168.57 cm^{-1} and 1041.27 cm^{-1} , attributed to C–O–C and C–O stretching, show minor changes, while the 610.14 cm^{-1} S–O bending vibration confirms the sulfonic acid group's integrity. All major peaks of SBE- β -CD are retained in the complex, albeit with decreased intensity and slight broadening, supporting the formation of a non-covalent host–guest inclusion complex. The absence of new peaks and preservation of SBE- β -CD's structure further confirm that complexation occurs via hydrogen bonding and hydrophobic interactions without chemical modification. These findings validate the formation of a stable inclusion complex through physical entrapment of valsartan within the cyclodextrin cavity.

SEM Analysis

The SEM image in Figure 7 reveals a rough, fibrous surface with an irregular texture, indicative of an amorphous or semi-crystalline matrix commonly seen in thin films designed for rapid drug release. This surface morphology increases the available surface area, which may enhance disintegration and dissolution rates. The pronounced irregularities are likely to promote faster hydration and erosion, facilitating rapid film disintegration upon contact with saliva.

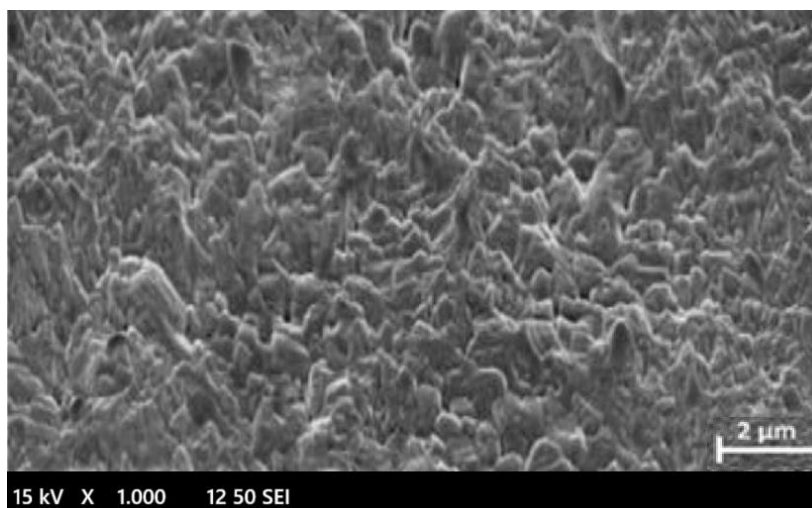


Figure 7: SEM image of Valsartan-SBE cyclodextrin inclusion complex OTFs

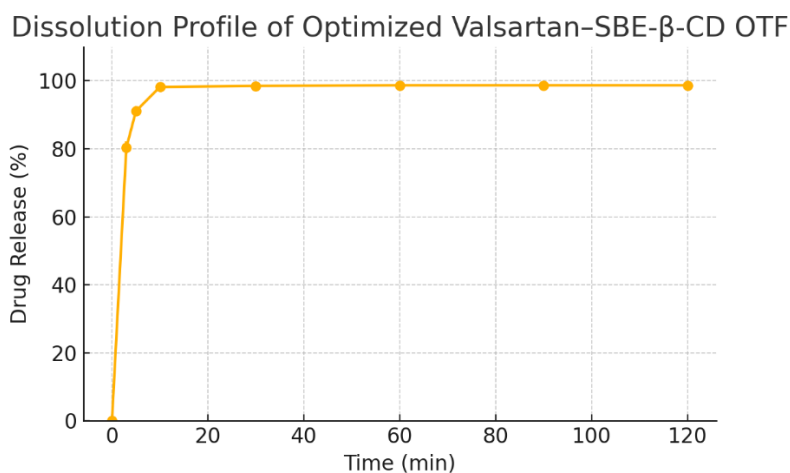


Figure 8: Dissolution profile of the optimized valsartan–SBE-β-cyclodextrin oral thin film.

Disintegration Time

Disintegration time (Response 3) showed substantial variation, ranging from 54 s (F13) to 113 s (F4). Higher polymer concentrations prolonged disintegration, as evident from F4 and F11, whereas formulations like F6 and F7 (0.8% polymer) disintegrated more rapidly (61–58 s). This behavior is consistent with the water-retaining capacity of hydrophilic polymers, which delays film erosion. Plasticizer had a less pronounced effect on disintegration time but contributed to uniform film morphology, indirectly aiding rapid disintegration at optimal levels.

Invitro Drug release

The dissolution profile of the optimized valsartan–SBE-β-cyclodextrin (SBE-CD) oral thin film (OTF), as presented in Table 5 and Figure 8, demonstrates a remarkably rapid and efficient drug release pattern. At the initial time point (0 min), no drug release was observed, confirming the absence of premature dissolution. However, within just 3 minutes, a significant release of $80.3\% \pm 1.87$ was recorded, indicating the film’s fast disintegration and effective wetting behaviour in the dissolution medium.

Table 5: Dissolution of Optimized OTFs

Time (mins)	Valsartan-SBE CD (Oral Thin Film)
0	0
3	80.3±1.87
5	91.1±1.42
10	98.2±1.06
30	98.5±0.97
60	98.7±1.03
90	98.7±0.85
120	98.7±0.79

By the 5-minute mark, the cumulative drug release increased to $91.1\% \pm 1.42$, suggesting that the majority of the drug had been released within the first few minutes. This rapid release is likely attributed to the amorphous or semi-crystalline



nature of the film matrix, as previously supported by SEM analysis, which enhances wettability and facilitates drug diffusion. The incorporation of SBE- β -cyclodextrin may have further improved the solubility of valsartan by forming an inclusion complex, thereby increasing its dissolution rate.

A near-complete release of $98.2\% \pm 1.06$ was achieved by 10 minutes, indicating that the formulation meets the requirements for rapid onset of action, which is ideal for orally disintegrating systems intended for immediate therapeutic effect. Beyond 10 minutes, the release profile plateaued, with values reaching $98.5\% \pm 0.97$ at 30 minutes and stabilizing at 98.7% through 60, 90, and 120 minutes with minimal standard deviation, suggesting the consistency and reproducibility of the drug release behaviour.

The rapid drug release observed is a favourable attribute for patient compliance, especially in populations requiring fast onset of action, such as hypertensive patients. The film's ability to disintegrate and release over 90% of the drug within 5 minutes also supports its potential for bypassing first-pass metabolism and enhancing bioavailability.

In summary, the dissolution data confirm that the optimized valsartan–SBE- β -cyclodextrin oral thin film (OTF) enables rapid, efficient, and consistent drug release, significantly enhancing the solubility and onset of action of poorly water-soluble drugs like valsartan. This formulation offers a patient-friendly dosage form specifically suited for pediatric use, providing fast disintegration, improved bioavailability, and ease of administration—effectively overcoming the challenges associated with conventional paediatric drug delivery systems.

CONCLUSION

This study successfully developed and optimized a novel orally dissolving thin film (OTF) containing valsartan complexed with sulfobutylether- β -cyclodextrin (SBE- β -CD) to address critical challenges in paediatric and post-myocardial infarction (MI) therapy. The phase solubility studies confirmed a remarkable 40.1-fold enhancement in solubility due to strong complexation ($K_{1:1} = 50.7 \text{ M}^{-1}$), ensuring adequate drug loading and rapid dissolution. The lyophilized inclusion complex (1:1.4 w/w valsartan: BE- β -CD) was effectively incorporated into OTFs using a solvent casting method, with pullulan and glycerol concentrations optimized via Central Composite Design (CCD) to achieve desirable mechanical properties (tensile strength: 22.42 MPa, folding endurance: 161 folds) and rapid disintegration (70 s). FTIR and SEM analyses confirmed successful drug-cyclodextrin complexation and uniform film morphology, while *in vitro* dissolution studies demonstrated >98% drug release within 10 minutes, ensuring rapid onset of action—a crucial factor for hypertensive emergencies and paediatric dosing. The formulation also inherently masked valsartan's bitterness through molecular encapsulation, eliminating the need for additional taste-masking agents. The developed valsartan-SBE- β -CD OTF presents a patient-centric, scalable, and clinically viable alternative to conventional tablets, particularly for paediatric and dysphagic post-MI patients who struggle with swallowing and medication adherence. By combining cyclodextrin-based solubility enhancement with OTF technology, this study bridges a significant gap in cardiovascular and paediatric drug delivery, offering a stable, palatable, and rapidly disintegrating dosage form that ensures accurate dosing, improved compliance, and enhanced bioavailability. Future work should focus on *in vivo* pharmacokinetic studies and long-term stability assessments to facilitate clinical translation.

ACKNOWLEDGEMENT

The authors are grateful to the Department of Pharmaceutics, Motherhood University, Roorkee, Uttarakhand, India, for providing the necessary facilities for the successful completion of this work.



AUTHOR CONTRIBUTION

All authors contributed equally with current work.

CONFLICT OF INTEREST

Authors disclose no conflict of interest with current work.

REFERENCES

1. Golhen, K., Buettcher, M., Kost, J., Huwylar, J., & Pfister, M. (2023). Meeting Challenges of Pediatric Drug Delivery: The Potential of Orally Fast Disintegrating Tablets for Infants and Children. *Pharmaceutics*, 15(4), 1033. <https://doi.org/10.3390/pharmaceutics15041033>
2. Domingues, C., Jarak, I., Veiga, F., Dourado, M., & Figueiras, A. (2023). Pediatric Drug Development: Reviewing Challenges and Opportunities by Tracking Innovative Therapies. *Pharmaceutics*, 15(10), 2431. <https://doi.org/10.3390/pharmaceutics15102431>
3. Flynn, J. T., Meyers, K. E., Neto, J. P., de Paula Meneses, R., Zurowska, A., Bagga, A., Mattheyse, L., Shi, V., Gupte, J., Solar-Yohay, S., Han, G., & Pediatric Valsartan Study Group (2008). Efficacy and safety of the Angiotensin receptor blocker valsartan in children with hypertension aged 1 to 5 years. *Hypertension (Dallas, Tex. : 1979)*, 52(2), 222–228. <https://doi.org/10.1161/HYPERTENSIONAHA.108.111054>
4. Baracco, R., & Kapur, G. (2011). Clinical utility of valsartan in the treatment of hypertension in children and adolescents. Patient preference and adherence, 5, 149–155. <https://doi.org/10.2147/PPA.S12166>
5. Kemna, M., Albers, E. L., Law, S. P., & Kemna, M. (2020). Valsartan/sacubitril in pediatric heart failure. *The Journal of Heart and Lung Transplantation*, 39(4), S364. <https://doi.org/10.1016/j.healun.2020.01.275>
6. Liu, Y., Wang, J., Wang, X., Liu, P., & Pang, F. (2009). Solubility of Valsartan in Different Organic Solvents and Ethanol + Water Binary Mixtures from (278.15 to 313.15) K. *Journal of Chemical & Engineering Data*, 54(3), 986–988. <https://doi.org/10.1021/je8007815>
7. Zhang, H., Zhang, Y., Xue, F., Chen, H., Gao, Z., Du, S., & Wang, Y. (2024). Insight into the dissolution behavior of valsartan (form E) in twelve pure solvents: Solubility, modelling and molecular simulation. *Journal of Molecular Liquids*, 402, 124774. <https://doi.org/10.1016/j.molliq.2024.124774>
8. Sevinç Özakar, R., & Özakar, E. (2021). Current Overview of Oral Thin Films. *Turkish journal of pharmaceutical sciences*, 18(1), 111–121. <https://doi.org/10.4274/tjps.galenos.2020.76390>
9. Yir-Erong, B., Bayor, M. T., Ayensu, I., Gbedema, S. Y., & Boateng, J. S. (2019). Oral thin films as a remedy for noncompliance in pediatric and geriatric patients. *Therapeutic delivery*, 10(7), 443–464. <https://doi.org/10.4155/tde-2019-0032>
10. Jacob S, Boddu SHS, Bhandare R, Ahmad SS, Nair AB. Orodispersible Films: Current Innovations and Emerging Trends. *Pharmaceutics*. 2023 Dec 11;15(12):2753. doi: 10.3390/pharmaceutics15122753. PMID: 38140094; PMCID: PMC10747242.
11. Pardeshi, C. V., Kothawade, R. V., Markad, A. R., Pardeshi, S. R., Kulkarni, A. D., Chaudhari, P. J., Longhi, M. R., Dhas, N., Naik, J. B., Surana, S. J., & García, M. C. (2023). Sulfobutylether- β -cyclodextrin: A functional biopolymer for drug delivery applications. *Carbohydrate Polymers*, 301(Part B), 120347. <https://doi.org/10.1016/j.carbpol.2022.120347>
12. dos Santos, C., Buera, M. d. P., & Mazzobre, M. F. (2011). Phase solubility studies of terpineol with β -cyclodextrins and stability of the freeze-dried inclusion complex. *Procedia Food Science*, 1, 355–362. <https://doi.org/10.1016/j.profoo.2011.09.055>
13. Wang, W., Tang, K., Huang, C., & Liu, A. (2024). Fabrication of sulfobutylether- β -cyclodextrin/glabridin inclusion complex for promoting bioactivities. *Archiv der Pharmazie*, 357(8), e2400082. <https://doi.org/10.1002/ardp.202400082>
14. Prajapati, V. D., Chaudhari, A. M., Gandhi, A. K., & Maheriya, P. (2018). Pullulan based oral thin film formulation of zolmitriptan: Development and optimization using factorial design. *International Journal of Biological Macromolecules*, 107(Part B), 2075–2085. <https://doi.org/10.1016/j.ijbiomac.2017.10.082>
15. Abdelhameed, A. H., Abdelhafez, W. A., Saleh, K. I., Hamad, A. A., & Mohamed, M. S. (2023). Formulation and optimization of oral fast dissolving films loaded with nanosuspension to enhance the oral bioavailability of Fexofenadine HCl. *Journal of Drug Delivery Science and Technology*, 85, 104578. <https://doi.org/10.1016/j.jddst.2023.104578>
16. El-Ansary AL, Salama NN, FM AA, Hassib HB, Mohamed MA. Validated spectrophotometric methods for determination of escitalopram through study of charge transfer and ion pair complexation. *J Chem Acta*. 2013; 2:119–28.
17. Prajapati VD, Chaudhari AM, Gandhi AK, Maheriya P. Pullulan-based oral thin film formulation of zolmitriptan: development and optimization using factorial design. *Int J Biol Macromol*. 2018;107(Pt B):2075–85. doi: 10.1016/j.ijbiomac.2017.10.082.
18. Kamali H, Farzadnia P, Movaffagh J, Abbaspour M. Optimization of curcumin nanofibers as fast dissolving oral films prepared by emulsion electrospinning via central composite design. *J Drug Deliv Sci Technol*. 2022; 75:103714. doi: 10.1016/j.jddst.2022.103714